ARTICLES

Detailed Study of Ice Clathrate Relaxation: Evidence for the Existence of Clathrate Structures in Some Water−Alcohol Mixtures

S. S. N. Murthy*

School of Physical Sciences, Jawaharlal Nehru University, New Delhi-110 067, India

Received: February 11, 1999

Dielectric relaxation technique (10^{+6}−10^{-3} Hz) and differential scanning calorimetry are used to study the existence of clathrate hydrates in aqueous solutions of a number of alcohols and non hydrogen-bonded liquids. The aqueous solutions studied are those of methanol, ethanol, 2-propanol, *tert*-butyl alcohol, acetone, and *p*-dioxane. The corresponding solid−liquid phase diagrams are also determined to support the dielectric results. Evidence for the existence of clathrate hydrates in 2-propanol and *tert*-butyl alcohol is provided. The clathrate hydrate of 2-propanol is metastable. No clathrate structure is found in methanol mixtures. The composition of the new clathrate found in 2-propanol and *tert*-butyl alcohol is suggested to be around A. $5H_2O$−A. $6H_2O$. The clathrate hydrate relaxation (including that of the two hydrates of ethanol) has been studied down to its kinetic freezing temperature T_g and is analyzed in terms of the Arrhenius equation. Also studied are the relaxation rates of the clathrate hydrates of acetone, tetrahydrofuran, and *p*-dioxane down to their respective T_gs. The nature of the dielectric relaxation is discussed.

Introduction

The study of physicochemical processes in mixtures of water with a variety of organic and inorganic liquids is of immediate relevance to many branches of chemistry and chemical technology. Apart from the work done on this front (for a review, see refs 1−4), the study of aqueous solutions is currently receiving a lot of attention[5−9] in view of the suspected micelle-like structures on the water-rich side which are considered as reference systems for more complicated aqueous systems such as surfactants, emulsions, and biopolymers. With this in mind, a lot of measurements have been reported in the past few years on the dielectric relaxation[10−16] and thermodynamic[6,7,17−20] properties. Also of interest in these systems on the application front are the phase studies involving binary and ternary solvent systems which are of immense use in various analytical techniques[1] and also in the low-temperature preservation of biological samples.[21,22] As is well-known, the solid water formed during the freezing of these systems at ordinary pressures can also exist in a cubic form in the form of clathrate hydrates I_c (or ice clathrates) besides the hexagonal ice I_h.[23−25] This area of clathrate hydrate research is again receiving attention because of its astrophysical[26,27] and biological implications.[12−15,17−23,28−32] It is interesting to see that the experimental results in the aqueous solutions of alcohols which are of biological significance are interpreted in terms of a clathrate (like) structure of composition of hexahydrates or pentahydrates. Hence, it is tempting to look at the corresponding solid−liquid phase diagrams which should reveal the presence of the clathrate structures. However, the existing experimental data on alcohols are not able to give the required information because of long crystallization times (see the Results section for details), and lamentable gaps exist in the study of these systems.

The voids in the clathrate hydrates are subject to attractive forces which will cause them to collapse unless the voids are occupied by the "guest" molecules. Because of the limitations on the size of voids, all sufficiently hydrophobic molecules with sizes less than 6.6 Å form clathrates (provided the molecule is not too small). Apart from the size, the chemical nature of the guest molecules also plays an important role. Approximately 100 clathrate hydrates are known so far, and interestingly, the guest molecules do not contain either a single strong hydrogen (H-) bond functional group (e.g., alcohols) or multiple H-bond functional groups (e.g., ethylene glycol[33,34]). Among the alcohols, ethanol[35−37] is the only alcohol which is found to be an exception to this rule. There is some ambiguity in the case of methanol[26] and in *tert*-butyl alcohol, although the solid−liquid phase diagram[35] indicates a clathrate structure which is yet to be confirmed by either dielectric spectroscopy or X-ray analysis.

There are seven predicted structures for the clathrate hydrates, where there is no H-bonding interaction between the guest species and the host framework.[24] With three exceptions, all known clathrate hydrates have either structure I or II or both. According to the survey conducted by Davidson,[23] molecules of diameter exceeding 5.8 Å are not known to form structure I clathrate hydrates. Ethanol, which has a free diameter of ∼6.6 Å forms two hydrates; the stable one is found to be type II and the other is found to be metastable whose composition is suggested to be closer to that of type I (however, a different view also exists on the exact nature of the stable clathrate[24,36]), but no details are available on the exact composition of type I clathrate. Similarly the suggested[35] clathrate structure of the hexahydrate of *tert*-butyl alcohol cannot be justified to be a type I clathrate in view of the large size of the *tert*-butyl alcohol molecule. It appears that we cannot rule out the possibility of

10.1021/jp990518t CCC: $18.00
Published on Web 09/17/1999

structures other than type I or II in the case of alcohols, but more information is required. (Sometimes the type II clathrate hydrate suggested by Potts and Davidson[35] is referred to as an "improper clathrate"[24] as the enclathrated molecules are not free to rotate inside the voids.)

Hence, a necessity is felt to critically examine the solid phase of the aqueous mixtures of alcohols using dielectric spectroscopy, for the possibility of clathrate hydrate relaxation. In this context, it is interesting to note that in some of the recent articles,[39,40] the kinetic freezing of the clathrate hydrate relaxation corresponding to some non H-bonding guest molecules is referred to as glass transition and the clathrate hydrates (above this transition temperature T_g) are referred to as plastic crystals because of disorder in the host lattice. In view of these reports we wish to critically examine the relaxation process of the clathrate hydrates to see whether there are any commonalities in the relaxation of clathrate hydrates and that occurring in plastic crystals.[41] We propose to do this by extending the measurements to ultralow frequencies in the dielectric relaxation technique.

Experimental Section

The water used in this study is of reagent grade deionized water and is obtained from M/s. Reckon Diagnostics Pvt. Ltd. India. The water obtained from M/s. E. Merck, of HPLC grade, is also used. Following are the details of the other liquids used in this study: (1) 2-propanol or 2POH (HPLC, M/s. E. Merck, India); (2) ethanol or EOH (AR Grade, M/s. E. Merck, Germany); (3) methanol or MOH (HPLC; M/s. S. D. fine Chem. Ltd., India); (4) 2-methyl-2-propanol or *tert*-butyl alcohol or tBOH (LR, M/s. S. D. fine Chem. Ltd.); (5) acetone or ACN (AR grade, from M/s. S. D. fine Chem. Ltd.); (6) *p*-dioxane or DXN (HPLC, M/s. CDH, India); (7) tetrahydrofuran or THF (HPLC, M/s. E. Merck, India).

For the present work, a DuPont 2000 Thermal Analyst system with quench cooling accessory has been used for differential scanning calorimetry (DSC) study and HP 4284A precision LCR Meter (frequency range 20 to 10^6 Hz) has been used for the dielectric study. For the dielectric measurements in the ultralow-frequency region of $10^{-0.85}$ -10^{-3} Hz, a dc step response technique is used.[43] The DSC cell is calibrated for the temperature using water and mercury, and for the cell constants at different temperatures using naphthalene, *o*-terphenyl, water, mercury, and *n*-pentane. Hermetically sealed sample pans made of aluminum weighing about 57 mg were used for DSC measurements (for further details of the DSC method, the reader may consult ref 42). The dielectric cell used in the study is made of nickel and is a two-terminal guarded electrode assembly. The temperature calibration and controlling, and the accuracy of the cell, etc., are the same as detailed before.[43]

Results and Analysis

Although our main aim is to study the dielectric relaxation of the clathrate hydrates, a necessity has been felt to make a systematic study of the solid−liquid-phase equilibrium to gauge the stability of various phases present during both the non-equilibrium and equilibrium conditions, although at first glance it may appear as if we have been measuring the same thing that is already known. In our measurements we have taken care of the time-dependent effects such as (i) crystallization, (ii) formation of clathrate structure for the hexagonal ice and remaining liquid, (iii) stability of the phases, and (iv) formation of the stable/unstable compounds. This has become possible by using the dielectric method in combination with the DSC technique.[34] Although, the DSC technique is very widely used for the determination of the solid−liquid phase diagram (PD) of aqueous solutions,[35,44−47] some researchers still have some reservations about the use of this technique for the PD study. Our earlier work[34] has shown that with aqueous solutions it is accurate to ±0.5 K for the onset of melting (eutectic or clathrate hydrate melting) but is less accurate for the liquidus melting. It is with this limitation that the DSC results have to be examined in addition to DSC's known drawback as a dynamic technique. For the equilibrium PD studies we have used the dielectric method,[34] where the completely crystallized sample is heated at an approximate rate of 0.25°/min during which the static dielectric ϵ ($-\epsilon'$ at 100 kHz test frequency) is monitored as a function of temperature from which the transition temperatures are measured.[34] In our experience this method gives an accuracy of melting to ±1 K in most of the cases. There are some advantages with this technique:[34] (i) complete crystallization can be ensured where ϵ_0 falls to 1.05 n^2_D on complete crystallization; (ii) the stability of the phases can be monitored by annealing the sample at intermediate temperatures; and (iii) the appearance of the liquid phase can be identified as a high-frequency dispersion.

Even with the above-said limitations of these techniques in the accuracy of the measured transition temperatures, the amount of information one gets with these techniques is so much that they have become indispensable for the present study.

Analysis of the Dielectric Spectra

It is well-known that the dielectric relaxation process of the clathrate hydrate has a typical Cole−Cole behavior[48] which is given by

$$\frac{\epsilon'(f) - \epsilon_\infty}{\epsilon_0 - \epsilon_\infty} = \left[1 + i\left(\frac{f}{f_m}\right)\right]^{\alpha-1} \tag{1}$$

where f_m is the peak loss frequency, f is the frequency, α is the symmetric distribution parameter, and ϵ_0 and ϵ_∞ are the low- and high-frequency limiting dielectric constants for the process under consideration. The temperature dependence of f_m in the "intrinsic" region usually follows[49] the Arrhenius form:

$$f_m = f_0 e^{(-E/RT)} \tag{2}$$

where E is the activation energy, and f_0 is the preexponential factor (often identified with the phonon frequency). The value of $\alpha = 0$ in eq 1 and the value of E is about 55.5 kJ/mol for hexagonal ice.[49] Using this as a guide, the relaxation behavior of the frozen samples is critically examined to determine the existence of clathrate hydrates. Sample-wise details of the results are included here.

(1) Water−2POH. From the PD study of Rosso and Carbonnel[44] and Ott et al.[38] it is not clear whether there is any ice clathrate (like) structure in this binary system.

Figure 1 shows the DSC curves taken during heating for the samples that were cooled normally (i.e., at a cooling rate of 5°−10°/min without annealing). One striking feature of these DSC curves is that in samples with mole fraction (x_m) ≥ 0.1 an additional endotherm is seen at 232 K which grows in size with x_m, but is diminished in size for $x_m \geq 0.19$. The endotherms shown at 175 and 222 K may be identified with the metastable eutectic and peritectic transitions given by Ott et al.[38] (see the PD of Figure 1).

Figure 2 shows the dielectric behavior of these samples in the above concentration range in the form of Cole−Cole

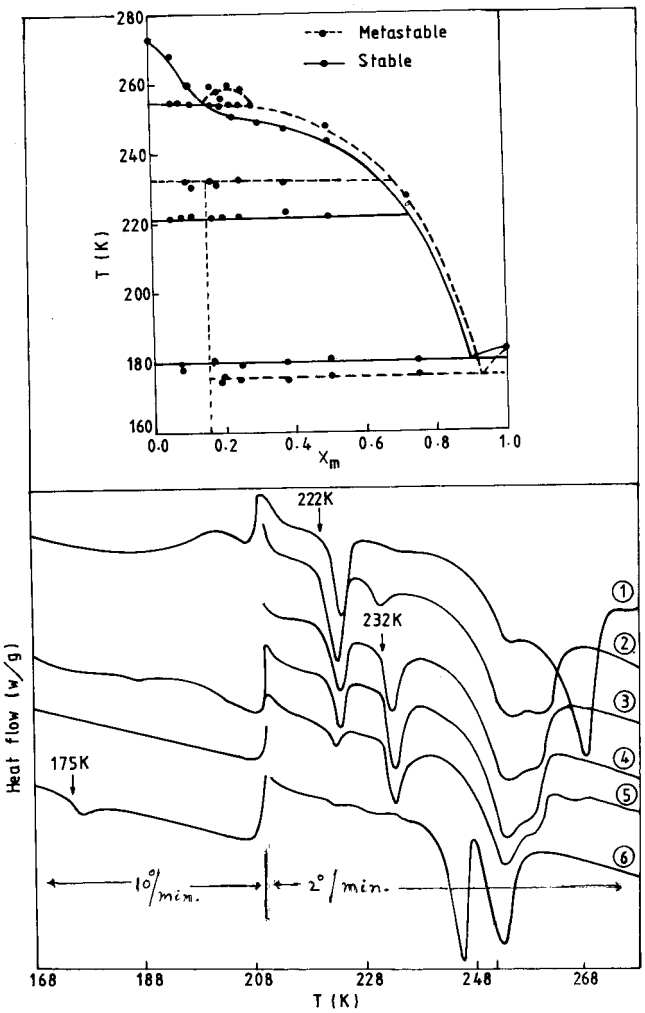

Figure 1. (Bottom) DSC thermograms taken during heating, for aqueous solutions of 2POH which were cooled at a rate of about 10°/min prior to the DSC run. The curves labeled correspond to (1) x_m = 0.07 (sample weight = 14.7 mg); (2) 0.111 (9.1 mg); (3) 0.135 (9.4 mg); (4) 0.148 (8.0 mg); (5) 0.191 (9.0 mg); and (6) 0.254 (10.5 mg). (Top) Also shown is the solid−liquid phase diagram of H_2O−2POH. The thick lines are drawn through, what are believed to be, the equilibrium points. Use is made also of the melting point data of Ott et al.[38] in drawing these lines. A vertical dashed line has been drawn at $x_m \sim 0.15$, to show the clathrate hydrate existence in the metastable state.

(C−C) diagrams. They clearly demonstrate a dispersion of the type given by eq 1. Note that this relaxation disappears for temperatures above 232 K indicating that the 232 K transition corresponds to a clathrate hydrate decomposition.

The stability of this clathrate structure was studied and represented in Figure 3, parts a and b. In Figure 3a the DSC scan and the dielectric behavior of the sample cooled normally is shown. Figure 3b gives the corresponding data for the same sample annealed above 232 K for a few hours. Note that the clathrate structure is absent in the latter sample. Another feature of interest in Figure 3a is that there is no sign of any liquid below 222 K as is seen from ϵ_∞ of the clathrate dispersion ($\sim$3.2) which is not too different from the value of 1.05 n^2_D where n_D is the refractive index. On the other hand, in the annealed sample shown in Figure 3b, some liquid is present above 179 K transition, which can be seen from the fact that there is a dispersion above (not below) 179 K typical of Cole−Davidson type characteristic of liquid relaxation (see ref 41 for the details). Thus, it is tempting to identify this 179 K transition with the

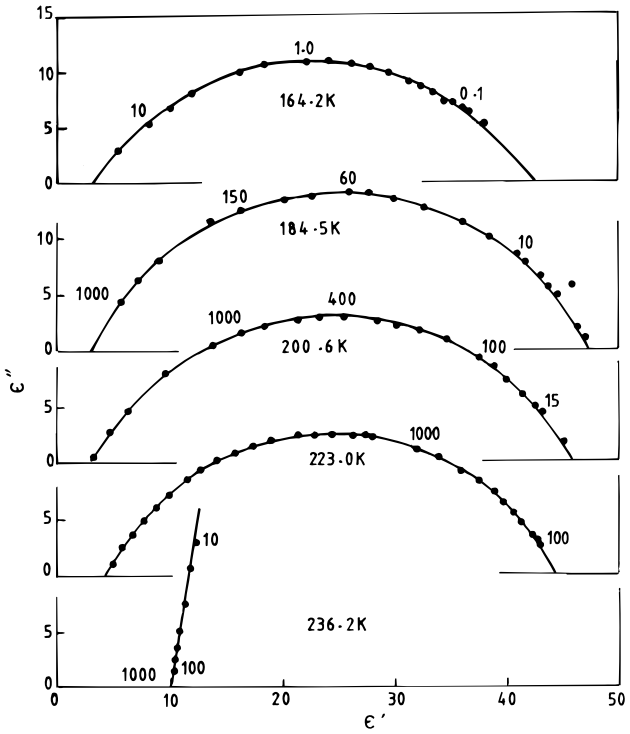

Figure 2. Cole−Cole diagrams showing the clathrate hydrate dispersion at different temperatures; in a sample of aqueous 2POH solution with $x_m = 0.1107$. (All the curves have the same ϵ' and ϵ'' scaling, but only the origin of these graphs is shifted vertically along the ϵ''-axis for the sake of clarity). Note the disappearance of the clathrate dispersion at 236.2 K. The numbers along the curves are the frequencies in KHz.

stable eutectic transition of Ott et al.[38] shown in the PD given in Figure 1. The details of our PD study are given in Table 1.

Figure 4 shows the temperature-dependence of the peak loss frequency f_m obtained by using eq 1, and the corresponding parameters of eq 2 are given in Table 2, for the intrinsic region.

Figure 5 depicts the temperature variation of the distribution parameter α.

(2) Water−EOH. Both the non-equilibrium[38,51] and the equilibrium PDs of this system are known. This system exhibits two ice clathrates[36,37] which are suggested[37] to be of the type I and II. The clathrate of type II is found to be stable[37] and has also been studied using dielectric spectroscopy.[35] However, the relaxation of the type I clathrate has not been studied previously and neither has the nature of the type II clathrate relaxation near its freezing temperature. We have filled this gap by studying the relaxation of both clathrates in detail. To ascertain ourselves about the stability of the clathrate structure, we have repeated the PD measurements for various cooling rates using the combination of dielectric and DSC methods. For this purpose the samples were annealed for a few tens of hours for crystallization separately in a dielectric cell and were then moved into the DSC cell at low temperature for the measurement of transition temperatures.

Figure 6a shows two DSC curves for the same sample, well annealed and fast quench-cooled, respectively. The dominant features for both the curves are three endotherms. The endotherm at 148.9 K is not present in the quench-cooled sample. In addition the endotherm at 200.7 K is diminished in size and two more prominent endotherms have appeared at 210.8 and 215.3 K. The endotherms at 244.9 and 255.7 K are the liquidus temperatures above which the samples are completely liquid in phase.

TABLE 1: Summary of the Main Features of the Dynamic Phase Diagram[a]

Sl. No.	second component	details of the ice clathrate		details of the eutectic transition		nature of the equilibrium phase diagram (PD)
		type	T_d (K)	T_e (K)	X_e approx.	
1	2POH	I(?)(M)	232.0	180.0		eutectic with peritectic transition at 222 K and 255 K
2	EOH	II(S)	199.5	150 ± 2	0.850	eutectic with incongruent melting at 199.5 K
		I(M)	210.4			
3	MOH			157 ± 1	0.850	eutectic with unstable 1:1 complex with an incongruent melting at of 171.5 K; no evidence of any ice clathrate
4	tBOH	I(?)(S)	266.5	264.6	0.075	complicated PD with evidence of complex formation at $x_m \cong 0.33$; on the water-rich side the PD is eutectic with incongruent melting transition at T_d
5	ACN	II(S)	253.2	177.5	0.98	eutectic with incongruent melting transition at T_d and transition at 258.2 K which is probably a peritectic
6	DIO	II(S)	259.7	257.1	0.165	eutectic with incongruent melting transition at T_d with solid−solid transition in dioxane at 272 K

[a] S: Stable; M: Metastable; T_d = decomposition temperature of the clathrate; T_e = eutectic temperature, X_e = eutectic concentration; ?: not certain.

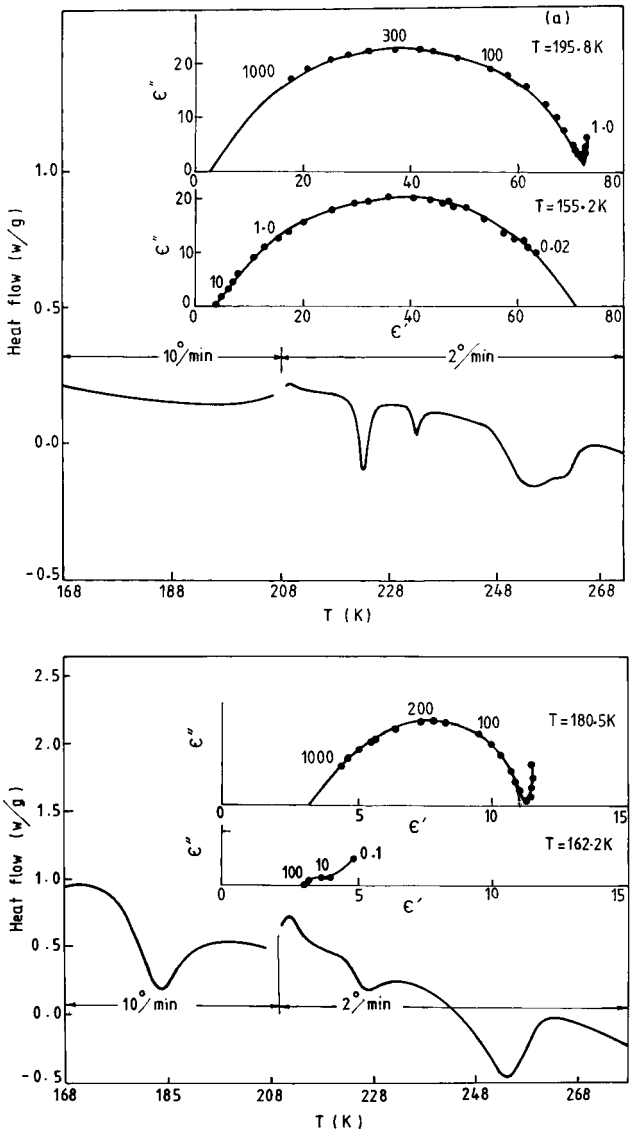

Figure 3. Water−2POH system with $x_m = 0.1679$. (a) DSC curve for a sample (of weight 10.9 mg) taken during heating after the sample was cooled at a rate of 10°/min. The inset shows the corresponding Cole−Cole diagrams showing the clathrate hydrate relaxation at temperatures above and below the equilibrium eutectic temperature of 179 K. Note the absence of the eutectic melting in both the techniques. (b) DSC curve for the sample which was very well annealed at different temperatures prior to cooling. Given in the inset are the corresponding Cole−Cole diagrams above and below the eutectic melting temperature of 179 K. Note the presence of liquid dispersion at 180.5 K (above the 179 K transition in the DSC curve).

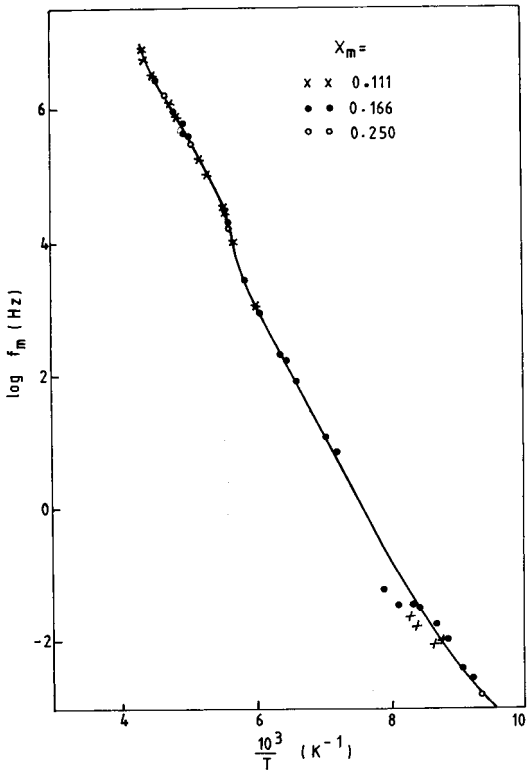

Figure 4. Arrhenius plot of f_m corresponding to the ice-clathrate hydrate relaxation in water−2POH system, for different x_m values. Note the "kink" on the curve.

TABLE 2: Details of Clathrate Hydrate Relaxation

	range of intrinsic relaxation (K)	T_d (K)	type of clathrate	log f_0 (Hz)	E (kJ/mol)
1. 2POH	182−231	232	I(?)	15.15	36.42
2. EOH	107−168	210.4	I(?)	16.27	38.66
	121−199	199.5	II	14.38	39.29
3. tBOH	242−261	266.5	I(?)	13.34	46.98
4. ACN	168−249	253.2	II	13.50	32.15
		−		(13.12[+])	(27.20[+])
5. DXN	214−256	259.7	II	13.373	39.63
	(200−256[+])			(−)	(38.10[+])

+ Literature values.[25,47,50]

From the previous work[35,37] it is inferred that in the case of well-annealed sample, the endotherm at 148.9 K is due to the eutectic melting and is split into two because of the presence of a small amount of hexagonal ice along with clathrate II which forms a separate eutectic with EOH. The endotherm at 200.7

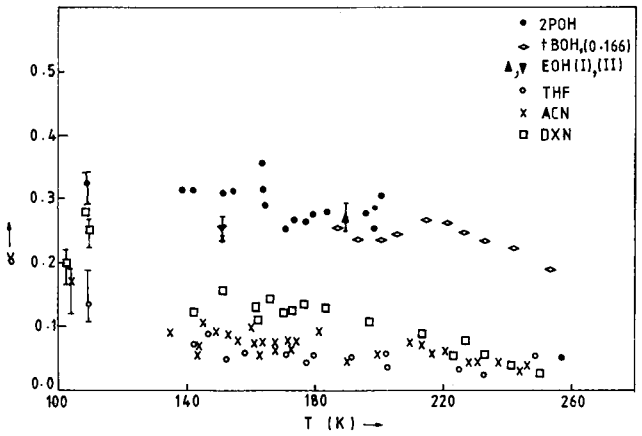

Figure 5. Variation of the parameter α of the clathrate dispersion with temperature for different systems.

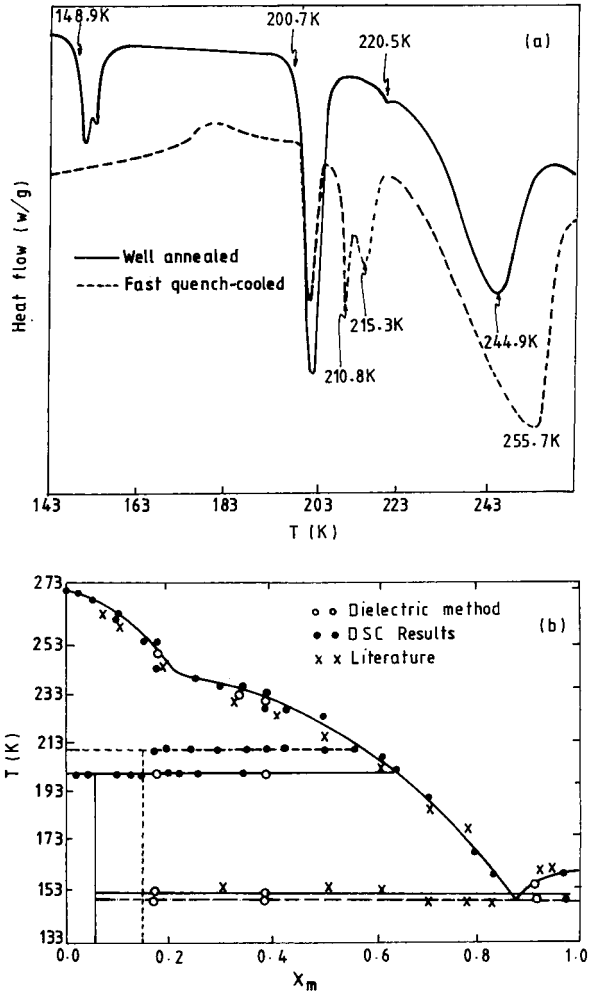

Figure 6. (a) Effect of the sample history on the DSC curves taken for a heating rate of 5°/min for water−EOH mixtures of concentration $x_m = 0.1752$. The sample labeled well-annealed is actually annealed for crystallization in a cryostat before it was shifted to the DSC cell at 100 K. (b) The phase diagram of water−EOH system. The points (•) shown along the dashed lines correspond to the various metastable transitions in the DSC scans. The open circles refer to the transition temperatures obtained (for partially crystalline samples) using the dielectric method. (The literature values are taken from ref 35,52). The vertical dashed line at $x_m \sim 0.15$ refers to the existence of a metastable clathrate I hydrate.

K is due to the decomposition of clathrate II hydrate to stable liquid and hexagonal ice. The quench-cooled sample does not show the eutectic melting because of lack of time for crystallization along the eutectic temperature due to rapid cooling. The exotherm around 175 K is due to the conversion of hexagonal ice to either of the two or both clathrate hydrates. Also it is noticed that the final melting (or liquidus melting) temperature is much higher than in the case of slowly cooled sample. The endotherm at 210.8 K is present only at higher concentrations, where it becomes increasingly stable toward higher concentrations. For concentration $x_m > 0.225$, the endotherm at 200.7 K is found to be absent in the DSC scans taken for samples cooled at a normal rate. Appearance of an endotherm at 200.7 K requires prolonged annealing at temperatures just below this temperature. The endotherm at 210.8 K appears to be due to the decomposition of the clathrate I structure. The metastable transition around 223 K is noticed to be present in samples with x_m in the range 0.2−0.4 (see Figure 6b). Also, two more transitions, at 237.5 and 244.5 K, are observed in a narrow concentration range around $x_m = 0.15$. (Similar observations were also made by Boutron and Kaufmann[37] which were ascribed to the disordered clathrate structures).

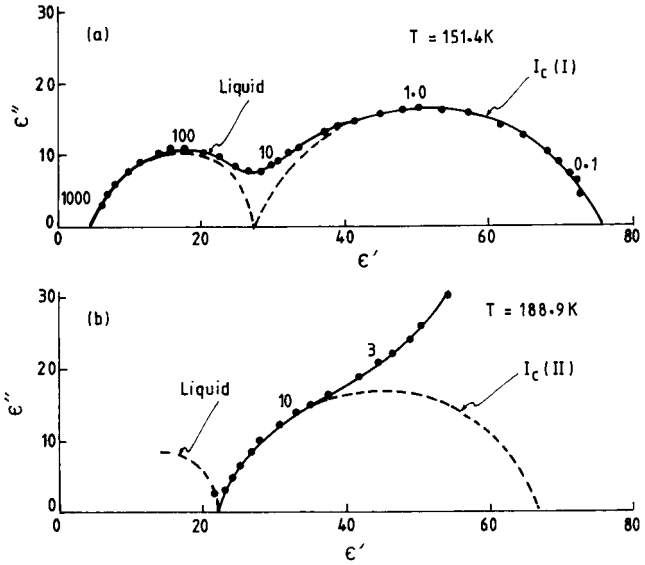

Figure 7. C−C plots for water−EOH system with $x_m = 0.405$. The number along the curves correspond to the frequency in KHz. (a) C−C plot showing the dispersion in the partially crystalline sample obtained by cooling at a rate of approximately 1°/min. Note the presence of both the liquid and the clathrate hydrate dispersions. (b) C−C plot for the same sample that was very well annealed for transformation of I_c (*I*) to I_c (*II*).

Figure 6b shows the PD for the water−EOH system which also reflects the transitions that have just been discussed. The stable transition temperatures were also confirmed by using the dielectric method[34] discussed in the previous sections and are also shown in the PD. (However, the transition temperatures corresponding to the disordered clathrate structure are not shown in the PD as these structures are probably not intrinsic in nature).

In Figure 7 are presented two C−C plots corresponding to two temperatures where the metastable clathrate I (top) and the stable clathrate (bottom) are in evidence in the sample with different thermal histories. The top graph is typical of the dielectric behavior of the normally cooled samples in the range $0.25 \leq x_m \leq 0.5$, where two relaxation processes can be observed.

From the shape of the corresponding C−C diagrams and with the help of the previous studies the higher frequency process is identified with liquid dispersion and the lower frequency process with clathrate I dispersion (Figure 7a). (Clathrate I is found to be stable enough for measurements to be taken down to its T_g).

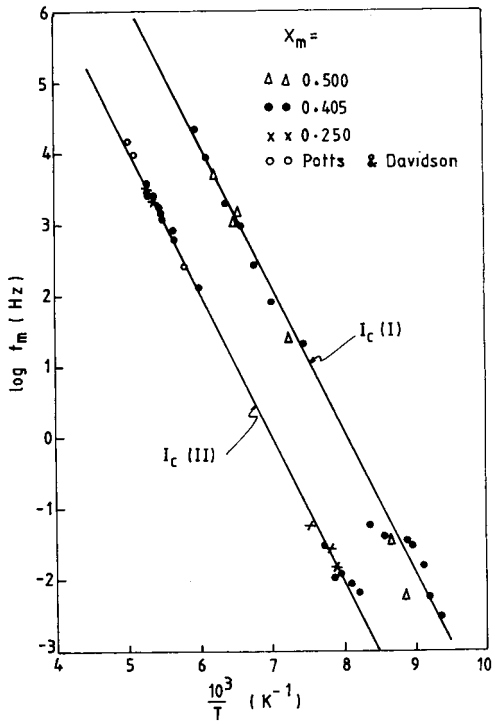

Figure 8. Arrhenius plot of f_m corresponding to the clathrate hydrate dispersions in water−EOH system. Also shown is the I_c (II) data of Potts and Davidson.[35]

However, at higher temperatures the two relaxations shown in Figure 7a merge with each other making the measurement of f_m difficult. Hence, the relaxation frequency corresponding to clathrate I could not be measured above 167 K. When the same sample is annealed around 199 K for 6 to 7 h, the dispersion of clathrate I disappears due to the collapse of clathrate I structure and a new dispersion appears in its place which may be identified with that of clathrate II (Figure 7b). The lower frequency spur shown in Figure 7b decreases in magnitude at lower temperatures, thus, facilitating the measurement of f_m without much problem.

Figure 8 depicts the temperature dependence of the f_m values thus measured for both the clathrates, and the corresponding parameters are given in Table 2.

(3) Water−MOH. The available PD[38,52] data on this binary points to a 1:1 compound formation, but what is not clear is whether there is any clathrate formation[26] or not. It is also not clear whether the existing PD data refers to an equilibrium situation or not. No dielectric relaxation measurements have been made so far to clarify the existence of clathrate hydrate.

Figure 9 (upper curve) shows the typical DSC scan for a completely crystallized sample of aqueous mixture of MOH on the water-rich side. The dominant features of the curves are the three endotherms.

Figure 9 (lower curve) depicts the temperature-variation of the static dielectric constant for the same sample. The three transition temperatures can be identified with the three endotherms of the DSC scan. Note the sample in Figure 9 is completely crystalline below 161 K transition, as can be seen from the fact that the dielectric constant is approximately close to the rigid crystalline value.

Figure 10a represents the stability of the phase below the lower endotherm at 161 K, where the partially molten sample was annealed around 167 K for a few (4−5) hours. For samples with $x_m < 0.50$, the samples again crystallize completely (as can be found from the corresponding ϵ' values in Figure 10a).

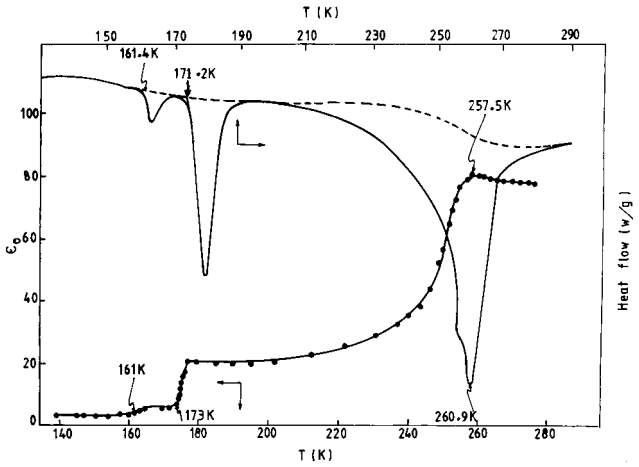

Figure 9. DSC curve for Water-MOH mixture of $x_m = 0.1354$ for a heating rate of 5°/min (upper curve). The dashed line is the sigmoidal baseline set by the software for the calculation of the transition temperatures. (The sample was crystallized in the dielectric cell before shifting it to the DSC cell at 100 K). The lower curve is the corresponding variation of the dielectric constant ϵ' at 100 kHz (approximately equal to the static dielectric constant of the liquid dispersion) in a constant rate of heat experiment.

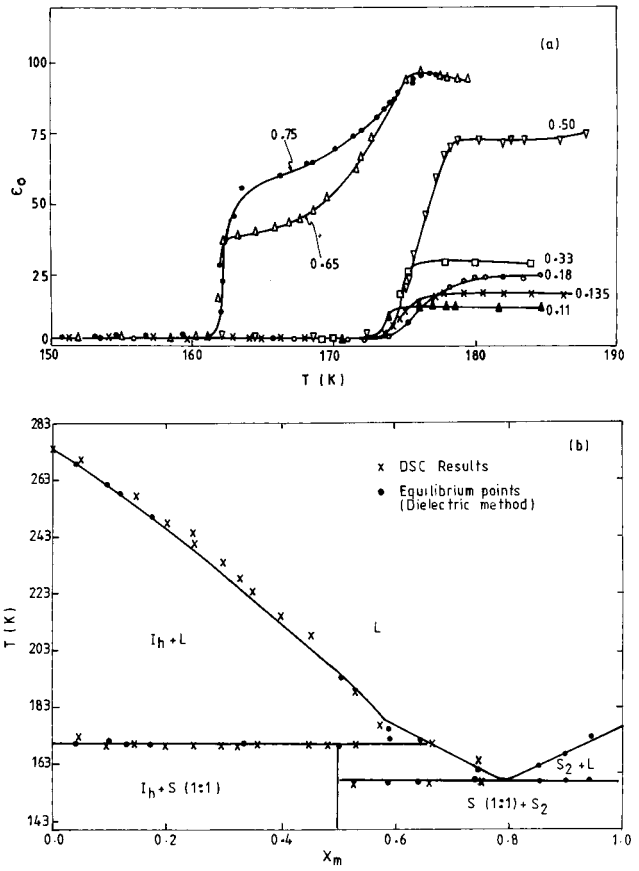

Figure 10. H_2O−MOH (a) Variation with temperature of the dielectric constant $\epsilon_0[= \epsilon'$ (100 kHz)] corresponding to the dipolar part, for completely crystallized and equilibrated samples in a constant rate of heat experiment in the region of the eutectic temperature. The curves correspond to different concentrations, as shown in the figure. Note the absence of eutectic melting at 161 K for $x_m \leq 0.5$. (b) The complete phase diagram. The points shown by the symbol (×) correspond to the DSC and those shown by the symbol (•) correspond to the dielectric (equilibrium) method. In the diagram S(1:1) corresponds to the 1:1 compound, S_2 corresponds to the solid MOH, and L stands for liquid.

This probably refers to the equilibrium situation. From Figure 10a, the absence of the melting transition at 161 K for samples

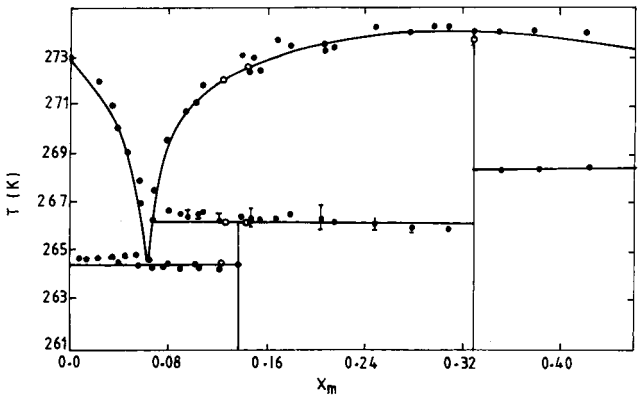

Figure 11. The phase diagram of Water-tBOH system shown for $x_m < 0.48$. The points shown correspond to •: DSC, °: dielectric method. The thick lines shown for liquidus lines correspond to the melting point data given by Ott et al.[38] The vertical line at $x_m \sim 0.15$ refers to the approximate composition of the stables hydrates.

with $x_m < 0.50$ may be noted. It is inferred that the lower endotherm at 161 K in Figure 9 corresponds to a non-equilibrium situation. Figure 10b, gives the complete details of our results in the form of PD.

Thus, it appears that the transition at 161 K is the eutectic temperature and that at 170.5 K is the incongruent melting (decomposition) temperature of the 1:1 compound. [For mixtures with $x_m > 0.3$, another endotherm in the DSC scans is observed during the course of investigation at temperatures around 175.5 K in addition to the incongruent endotherm at 170.5 K. The former is found only in the rapidly cooled samples with x_m above 0.3 (and hence is not shown in Figure 10b). The origin of this transition could not be ascertained].

We have critically examined the dielectric spectra of these mixtures at various concentrations and for non-equilibrium as well as equilibrium conditions. We have failed to notice any relaxation in the frequency range 10^6 to 10^{-3} Hz, that can be ascribed to a clathrate hydrate. For completely crystallized samples, the dielectric loss showed low-frequency spurs characteristic of space-charge or Maxwell−Wagner polarization. There was no sign of clathrate hydrate dispersion.

4. Water−tBOH. This binary system assumes a lot of significance in view of the reports of the existence of clustering of molecules in the liquid state. Two critical regions are identified: for $x_m < 0.05$, a cluster of the type tBOH $(H_2O)_n$ is suggested,[6] and change in the mixing scheme is proposed for $x_m > 0.05$. However, there is a disagreement[19,30,31] about whether these clusters are of a fixed value for n to have a clathrate-hydrate-like structure or not, and there is also a suggestion[19] of clustering of the type $5\{(H_2O)_{21}$ tBOH$\}$ for $0.05 < x_m < 0.16$. The dielectric relaxation study of these solutions by Mashimo and Miura[14] also reveal two critical concentrations of 0.03 and 0.17 which are again attributed to different types of clustering. These reports have tempted us to study the dielectric relaxation of the solid phase of these mixtures to verify the existence of a clathrate hydrate (like) structure. To facilitate our interpretation of the dielectric results, we have also critically examined the PD for the region $x_m < 0.44$ using both the DSC and dielectric methods although the information on PD is already available.[38,45]

Figure 11 shows the results of our DSC and dielectric method in the form of PD.

During the course of the investigation using DSC, we have noticed a slight change, by about 0.4 K, in the onset temperature of the lowest transition at 264.6 K for concentrations $x_m < 0.058$.

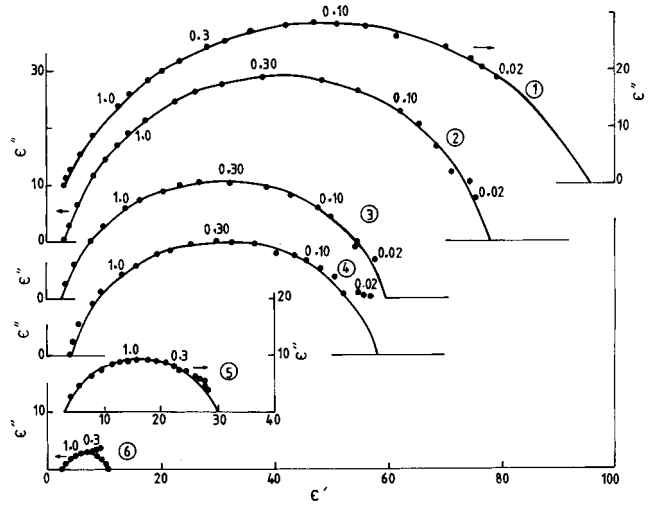

Figure 12. C−C plots obtained in the solid phase of water−tBOH system of different x_m's. The numbers by the side of the curves correspond to the frequencies in kHz and the thick line corresponds to the fits to eq 1. The curves numbered correspond to (1) $x_m = 0.015$, $T = 225.2$ K, $\alpha = 0.311$; (2) 0.0578, 224.7 K, 0.156; (3) 0.100, 221.2 K, 0.194; (4) 0.143, 225.7 K, 0.156; (5) 0.167, 227.2 K, 0.244; (6) 0.25, 225.8 K, 0.290.

But we are not very sure whether this change is really significant as it is comparable to the experimental uncertainity. This needs to be confirmed by other accurate measurements. It is also noticed in our DSC scans that for samples with $x_m > 0.1$, an endotherm at 266.5 K develops which increases in magnitude toward $x_m \sim 0.143-0.166$, beyond which it decreases and disappears altogether for $x_m \geq 0.33$. The eutectic transition at 264.6 K decreases in magnitude for $x_m > \sim 0.1$ and disappears around 0.143−0.166. At a concentration of $x_m = 0.33$ only one endotherm located around 273.4 ± 0.5 *K* has been noticed indicating a stable 2:1 compound of H_2O and tBOH. Thus, it appears that there is an incongruently melting hydrate corresponding to $x_m = 0.143-0.166$ in addition to a stable compound at $x_m = 0.33$. These observations are in general agreement with those of the earlier reports.[38,45]

Using the dielectric relaxation technique, the samples at 10 concentrations in the range of $0.015 \leq x_m \leq 0.33$, have been critically examined after proper annealing and thermal recycling below 265 K. Very broad C−C arcs are obtained for the relaxation in the solid phase. For a comparison, the shape of these plots at the same temperature (of around 225 K) but for different concentrations, are shown in Figure 12. For lower concentrations, especially for $x_m \leq 0.055$, the C−C plots are found to be slightly flatter than what is expected based on eq 1, and in order to get f_m values we had to force-fit the experimental values to eq 1. It appears as if the C−C plots for $x_m < 0.143-0.1665$ are a superposition of two relaxation processes of nearly the same relaxation frequency. A significant feature of our study is that for $x_m \geq 0.143-0.166$, all the dispersion is found to be associated with the 266.5 K transition (see Figure 11), above which the dispersion was found to disappear. Another significant feature of our study is that the magnitude of this clathrate (like) relaxation disapppears for $x_m \geq 0.33$, confirming a 2:1 compound formation of water and tBOH. Thus, it appears to us that the transition at 264.6 K is due to the eutectic melting of water and the incongruently melting clathrate hydrate.

Figure 13 shows the temperature-variation unresolved relaxation frequency; it clearly shows that all the curves converge at higher temperatures (we believe this to be the intrinsic region)

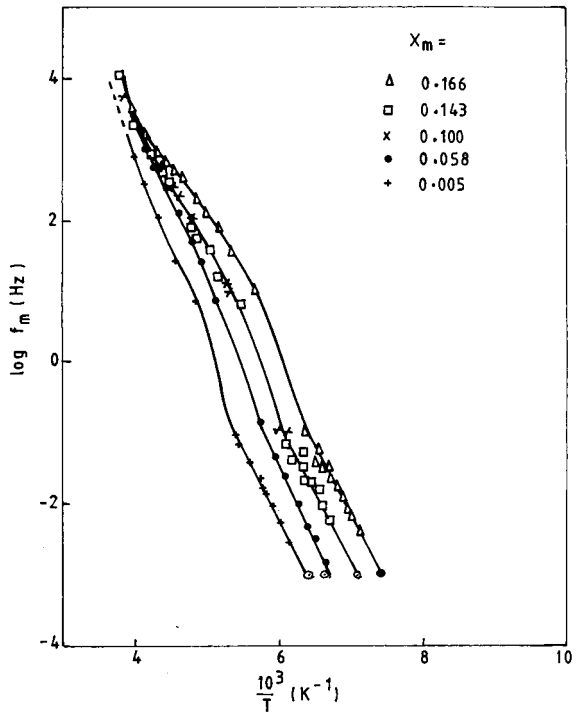

Figure 13. Arrhenius plots of f_m measured for the solid phase at several concentrations of the system water−tBOH. Also shown in the curve are the high-temperature data corresponding to hexagonal ice[49] (dashed line).

which is closer to that of hexagonal ice. The Arrhenius parameters for this relaxation are given in Table 2. We have also noticed that the kinetic freezing of the relaxation processes shown in Figure 13 corresponds to a small steplike change in the DSC curve, similar to that observed for the secondary relaxations in organic glasses.[54]

5. Water−ACN. The complete PD was determined by Wilson and Davidson[47] using thermal analysis and dielectric technique. However, the details of the thermal analysis are not given clearly. In this study the thermal behavior of these mixtures is critically examined over the entire concentration range.

Figure 14a shows the summary of the DSC results of the annealed samples in the form of PD. (In addition to the endothermic transitions shown in Figure 14a, a small exothermic peak with an enthalpy of transition of ∼2.5 J mol was noticed during the first heating of the samples in the DSC cell. This feature was not found during subsequent runs of the annealed samples. This feature is clearly due to the conversion of hexagonal ice into ice clathrate.

The endotherm at 177.7 K is not seen for concentrations less than 0.055 in well-annealed samples. This value of 0.055 for x_m refers to the clathrate hydrate II composition which is *A*. $17H_2O$[23] (where *A* is the second-component molecule). These observations are similar to that given in ref 47. However, some additional features are observed for samples annealed for much longer time. At this point our PD is very similar to the one suggested by Wilson and Davidson[47] except for a small additional feature at 258.2 K (Figure 14b). In the samples that are cycled between 163 and 213 K for about 6 to 7 h, one additional peak around 258.2 K is found in the DSC thermograms (Figure 14b). Shown in the same figure is the corresponding dielectric behavior which clearly shows both transitions.

Shown in Figure 15 are the f_m values obtained using eq 1, corresponding to the clathrate II dispersion found in the annealed

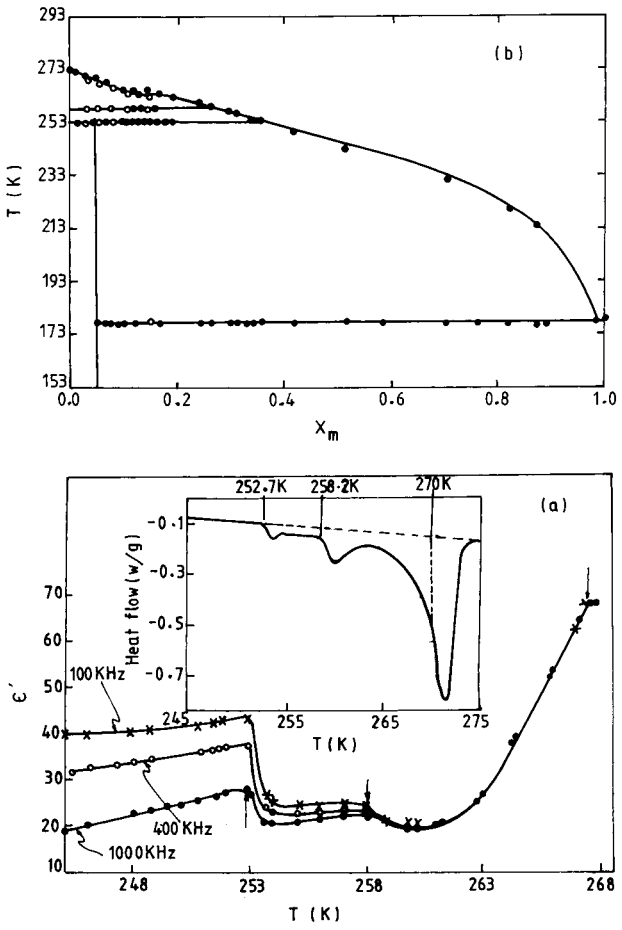

Figure 14. Water−ACN system. (a) The solid−liquid phase diagram. The open circles are for very well annealed samples as in (a). The closed circles correspond to the less-annealed samples. (b) Variation of ϵ' at various frequencies with temperature in the region of the clathrate hydrate melting for a well-annealed sample of $x_m = 0.055$. Shown in the inset is the corresponding DSC scan for a heating rate of 1°/min for the same sample taken from the dielectric cell of the cryostat. The transition temperatures in the dielectric property are indicated by arrows on the curves.

samples, and these values are found to be in good aggrement with the corresponding data by Davidson et al.[47,50]

It may be noted that the dispersion in ϵ' does not disappear totally above 253.2 K corresponding to the clathrate II decomposition (see Figure 14b). Because of this feature, we have critically examined the dielectric behavior of the samples at the concentrations between $x_m = 0.0154$ to 0.350. We have not found evidence for any relaxation process other than the one that can be ascribed to clathrate II and, hence, it is believed that the transition shown at 258.2 K corresponds to an event other than a (different) clathrate decomposition.

(6) Water−DXN. The PD of this system was published for the water-rich side by Nakayama[46] which clearly revealed the existence of a clathrate II hydrate. The dielectric relaxation of this hydrate was also studied.[55(b)] However, these measurements were not extended to the lower-temperature side.

We have studied the PD of this system over the entire concentration range using both DSC and dielectric methods. These results are entered in Table 1 and are similar to those of Nakayama.[46] (However, Nakayama did not study the PD on the DXN-rich side).

Given in Figure 16 are our f_m values corresponding to the clathrate II dispersion down to its kinetic freezing temperatures. The corresponding parameters α are given in Figure 5 along

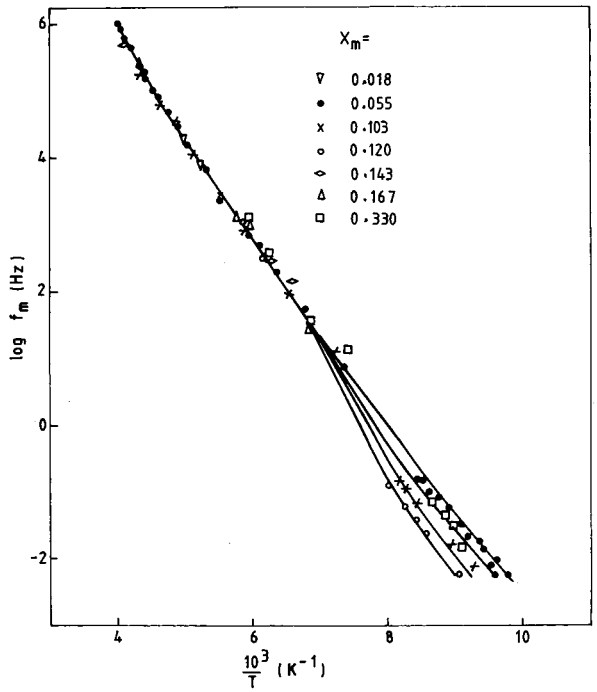

Figure 15. Arrhenius plot of f_m of clathrate hydrate relaxation, measured at different concentrations in Water-ACN system.

with that of the other systems. The other details of the hydrate relaxation are given in Table 2.

Out of curiosity, the clathrate II relaxation of the water−THF system was also studied at a concentration corresponding to the clathrate composition down to its freezing temperature (T_g). The details of the f_m values (along with the high-temperature published values[56]) are shown in Figure 16 and the corresponding α value is entered in Figure 5.

In addition, included in Figure 16 are the clathrate relaxation data of ACN discussed in the previous paragraph and also that of ethylene oxide studied by Davidson and Wilson[55] along with the dielectric data[56] on THF and the enthalpy relaxation data[39,40] of others for comparison purposes.

Discussion

(1) Composition of the Clathrate Hydrate. It appears that the composition of the clathrate hydrate of 2POH and tBOH lies around $x_m = 0.14-0.17$ corresponding to that of penta- or hexahydrates. This can be seen from the fact that the strength ($\epsilon_0 - \epsilon_\infty$) of the dielectric dispersion of the hydrate reaches a maximum around these concentrations (see Figures 2, 3, and 12). To assign an exact hydrate composition based on our study is not possible for the case 2POH and EOH (hydrate I) because of the unstable nature of these hydrates which interferes with the accuracy in the measured dielectric strength of the clathrate dispersion. These clathrate hydrates have an ϵ_∞ value of 3.2−3.5 (Figures 2, 3, and 12) which is not too different from the rigid lattice value of ∼1.05 n^2_D, indicating that the guest alcohol molecule is probably H-bonded to the host lattice and, hence, cannot rotate independently of the host lattice molecules. (This was shown to be the case with the structure II hydrate of ethanol which was studied in better detail by Potts and Davidson[35]). The large α -values for alcohol hydrates shown in Figure 5 are probably a result of a large number of defects[57−61] introduced by the guest molecules which are believed to be responsible for the reorientation of the water molecules. However, if the sizes of 2POH and tBOH are taken into consideration, these

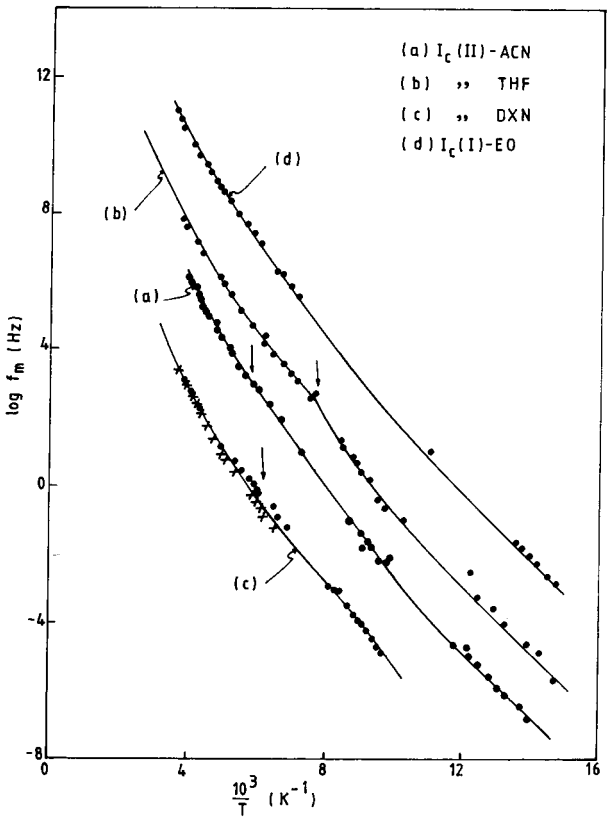

Figure 16. Arrehenius plots of f_m of clathrate hydrate relaxation measured at concentrations corresponding to the clathrate composition in non H-bonded systems. Also shown in the figure are the points corresponding to the enthalpy relaxation data[39,40] at temperatures below ∼80 K. (The "kinks" on the curves are shown by arrows.) The curves correspond to the clathrate hydrate of (a) ACN, (b) THF, (c) DIO, [the points (×) correspond to the data taken from ref 55(b)], and (d) EO[55(a)]. The curves (b), (c), and (d) are shifted along the log f_m axis by +2, −2, and +4 units, respectively, for the sake of clarity.

molecules are too large to fit into a clathrate I structure. Thus, it appears that the clathrate structure referred to as type I above is probably different from both I and II hydrates.

(2) H-Bonding Capability and Clathrate Formation. Interesting correlation between H-bonding capability and clathrate formation can be noticed in our study. MOH which is capable of forming stronger H-bonds with water than EOH (because of its size and lesser steric hindrance to the −OH group), does not form clathrates; instead it prefers a 1:1 compound formation with water. In this context, we have investigated the behavior of 1-propanol at $x_m = 0.143$ and 0.33, but found no evidence of clathrate structure (this is a preliminary investigation); whereas 2-propanol with its −OH group blocked by the neighboring $-CH_3$ groups forms slighty weaker H-bonds with water as compared to 1-propanol which, interestingly, is a clathrate former. Similar correlation exists among the ACN ($(CH_3)_2C{=}O$) and dimethyl sulfoxide ($(CH_3)_2S{=}O$) where, in the latter molecule, the $-S{=}O$ group is known to form stronger H-bonds than the $-C{=}O$ group with water molecules.[33,34] ACN forms structure II hydrate (Figure 14b) whereas clathrate structure does not exist in the latter, and in fact, DMSO forms two compounds with water[33,34] in the solid phase. Similarly the clathrate-forming capability of EOH vanishes if one H atom is replaced by a −OH group. This is the case of ethylene glycol which forms a 1:1 compound with water in the solid phase.[33,34]

(3) Dielectric Relaxation and the Shape of log f_m vs 1/T Curves. The most successful mechanism proposed to account for reorientation of water molecules in ice is that of Bjerrum[57−59,61]

and is adopted for ice clathrate relaxation as well.[23,60] In this model, the defect generated intrinsically by thermal excitation of the normal water molecule affects the reorientation of many water molecules before it is annihilated by an encounter with a defect of the complementary kind. However, disruption or distortion of the H-bonding around impurities and crystal imperfections may introduce extrinsic defects into the lattice in sufficient numbers so as to considerably accelerate the relaxation rate of the molecules which are many molecular diameters removed from the injection sites. These extrinsic defects are likely to control the relaxation at lower temperatures and one can expect deviations in linear log f_m vs $1/T$ curves as in Figure 16; *i.e.*, deviations from eq 2. The corresponding α value in eq 1 will then increase on lowering the temperature as shown in Figure 5. One significant observation here is that too much of a deviation from eq 2 is not observed for the relaxation in alcohols (see Figures 4 and 8) down to their kinetic freezing temperatures, T_gs, with the exception of tBOH (Figure 13). This can be understood in terms of extrinsic defects generated by the caged alcohol molecule, which is expected to have a stronger influence on the relaxation than the extrinsic defects generated by the imperfections. In nonalcoholic systems such as ACN, DXN, THF, and EO, there is a significant curvature in the log f_m vs $1/T$ curves which can be understood as due to the extrinsic defects generated by the grain boundaries or imperfections of other type, dominating the relaxation process at lower temperatures.

Another significant feature of the relaxation, is the small "kinks" in the log f_m vs $1/T$ curves in Figures 4 and 16 which become more prominent when the clathrate relaxation is measured in a mixture at a concentration different from that of the clathrate composition. This situation is demonstrated in Figure 15 in the case of ACN. When the extrinsic defect-diffusion mechanism is operational one can expect the environment around the clathrate "crystallite" to influence log f_m vs $1/T$ curves, especially, below T_e (the eutectic temperature) if the sample concentration x_m is different from that which corresponds to the clathrate composition because of the eutectic freezing. In fact, one can expect a steplike change in the environment around the "crystallite" and, hence, a steplike change in log f_m vs $1/T$ curves near T_e. Thus, the kinks can be due to a switching-over of one type of extrinsic mechanism to another.

Conclusions

(**1**) We have furnished evidence for the existence of clathrate hydrates in two more alcohols other than EOH. If these hydrates are of Type I, then the evidence suggests that the structure must be highly distorted. This conclusion is supported by the observed dependence of the clathrate-forming capability on the H-bonding capacity of the guest alcohol, by the large values of α, by the composition, and by the stability of the clathrates.

(**2**) The shape of the relaxation spectra, the observed dependence of activation energy E on temperature, and the extrinsic defect-dominated mechanism for relaxation on the lower-temperature side suggest that the freezing of the relaxation process cannot be compared to a glass transition event similar to those found in liquids or plastic crystals. Rather it is a "simple" kinetic event, even though it is tempting to identify the clathrate hydrate as a "strong glass"[41,62] on the basis of the change[39,40] in specific heat at T_g which is very small.

(**3**) In the case of tBOH and also EOH there seems to be some correlation between the observed liquid-state clusters[12−14,17−20] and the ice-clathrate structure in the solid phase. This does not seem to be true for MOH.

References and Notes

(1) *Water*: *A Comprehensive Treatise*, Vol 1−5; Franks, F., Ed.; Plenum Press: New York, 1973.
(2) *Physico-Chemical Processes in Mixed Aqueous Solvents*; Franks, F., Ed.; Heinemann Educational Books Ltd.: London; p 50.
(3) Angell, C. A. *Rev. Phys. Chem.* **1983**, *34*, 593.
(4) Hasted, J. B. *Aqueous dielectrics*; Chapman and Hall: London, 1973.
(5) *Micellization, Solubilization and Microemulsions*, Vol.1; Mittal, K. L. Ed.; Plenum Press, New York, 1977.
(6) Roux, G.; Perron, G.; Desnoyers, J. E. *J. Phys. Chem.* **1978**, *82*, 966.
(7) Koga, Y.; Siu, W. Y. W.; Wong, T. Y. H. *J. Phys. Chem.* **1990**, *94*, 3879.
(8) Myers, D. *Surfactant Science and Technology*; VCM Publ.: New York, 1988.
(9) D'Arrigo, G.; Texieira, J.; Giordano, R.; Mallamace, F. *J. Chem. Phys.* **1991**, *95*, 2732.
(10) Kaatze, U.; Pottel, R.; Schafer, M. *J. Phys. Chem.* **1989**, *93*, 5623.
(11) Kaatze, U.; Pottel, R.; Schmidt, P. *J. Phys. Chem.* **1988**, *92*, 3669.
(12) Mashimo, S.; Umehara, T.; Redlin, A. *J. Chem. Phys.* **1991**, *95*, 6257.
(13) Mashimo, S.; Miura, N.; Umehara, T.; Yagihara, S.; Higasi, K. *J. Chem. Phys.* **1992**, *96*, 6358.
(14) Mashimo, S.; Miura, N. *J. Chem. Phys.* **1993**, *99*, 9874.
(15) Tabellout, M.; Hanceleur, P., Emery, J. R.; Hayward, D.; Pethrick, R. A. *J. Chem. Soc., Faraday Trans.* **1990**, *86*, 1493.
(16) Puranik, S. M.; Kumbharkhane, A. C.; Mehrotra, S. C.*J. Chem. Soc., Faraday Trans.* **1992**, *88*, 433.
(17) Perron, G.; Desnoyers, J. E. *J. Chem. Thermodyn.* **1981**, *13*, 1105.
(18) Perron, G.; Couture, L.; Desnoyers, J. E. *J. Soln. Chem.* **1992**, *21*, 433.
(19) Koga, Y.; Wong, T. Y. H.; Siu, W. W. Y. *Thermochim. Acta* **1990**, *169*, 27.
(20) Koga, Y.; Siu, W. W. Y.; Wong, T. Y. H. *J. Phys. Chem.* **1990**, *94*, 7700.
(21) Nemethy, G. *Cryobiology* **1966**, *3*, 19.
(22) Ashwood, M. J.; Farvant, J. *Low-Temperature Preservation in Medicine and Biology*; University Park Press: Baltimore, 1980.
(23) Davidson, D. W. *Water*: *A Comprehensive Treatise*, Vol. 2: Franks, F., Ed.; Plenum Press: New York, 1973; p 115.
(24) Jeffrey, G. A. *Inclusion Compounds I*; Academic Press: London, 1984; p 135.
(25) Davidson, D. W.; Ripmeester, J. A. *Inclusion Compounds III*; National Research Council of Canada, 1984, p 69.
(26) Blake, D.; Allamandola, L.; Sanford, S.; Hudgins, D.; Freund, F. *Science* **1991**, *254*, 548.
(27) Mayer, E.; Hallbrucker, A. *Nature* **1987**, *325*, 601.
(28) Franks, F. *J. Soln. Chem.* **1995**, *24*, 1093.
(29) Hallbrucker, A. *Angew. Chem., Int. Ed. Engl.* **1994**, *33*, 691.
(30) Cowie, J. M. G.; Toporowski, P. M. *Can. J. Chem.* **1961**, *39*, 2240.
(31) Iwasaki, K.; Fujiyama, T. *J. Phys. Chem.* **1979**, *83*, 463.
(32) Higashigaki, Y.; Christensen, D. H.; Wang, C. H. *J. Phys. Chem.* **1981**, *85*, 2531.
(33) Murthy, S. S. N. *J. Phys. Chem.* **1997**, *101*, 6043.
(34) Murthy, S. S. N. *Cryobiology* **1998**, *36*, 84.
(35) Potts, A. D.; Davidson, D. W. *J. Phys. Chem.* **1965**, *69*, 996.
(36) Calvert, D.; Srivastava, P. *Acta Crystallogr. A* **1969**, *25*, 5131.
(37) Boutron, P.; Kaufmann, A. *J. Chem. Phys.* **1978**, *68*, 5032.
(38) Ott, J. B.; Goates, J. R.; Waite, B. A. *J. Chem. Thermodyn.* **1979**, *11*, 739.
(39) Kuratomi, N.; Yamamuro, O.; Matsuo, T.; Suga, H. *J. Chem. Thermodyn.* **1991**, *23*, 485.
(40) Yamamuro, O.; Oguni, M.; Matsuo, J.; Suga, H. *J. Phys. Chem. Solids* **1988**, *49*, 425.
(41) Murthy, S. S. N. To be published.
(42) Murthy, S. S. N.; Arya, N.; Paikaray, A. *J. Chem. Phys.* **1995**, *102*, 813.
(43) Murthy, S. S. N. *J. Phys. Chem.* **1996**, *100*, 8508.
(44) Rosso, J. C.; Carbonnel, L. *C. R. Acad. Sci. Paris-C* **1969**, *268*, 1012.
(45) Rosso, J. C.; Carbonnel, L. *C. R. Acad. Sci. Paris-C* **1968**, *267*, 4.
(46) Nakayama, H.; Tahara, M. *Bull. Chem. Soc. Jpn.* **1973**, *46*, 2965.
(47) Wilson, G. J.; Davidson, D. W. *Can. J. Chem.* **1963**, *41*, 264.
(48) Cole, K. S.; Cole, R. H. *J. Chem. Phys.* **1941**, *9*, 341.
(49) Von Hippel, A. *IEEE Trans. Electron. Insul.* **1988**, *23*, 801.
(50) Morris, B.; Davidson, D. W. *Can. J. Chem.* **1971**, *49*, 1243.
(51) Vuillard, G.; Satragno, N. *Compt. Rend.* **1960**, *250*, 3841.

(52) Timmermans, J. *The Physico-Chemical Constants of Binary Systems in Concentrated Solutions*, Vol. 4; Int. Sci. Publ.: New York, 1960.
(53) Ross, H. K. *Ind. Eng. Chem.* **1954**, *46*, 601.
(54) Murthy, S. S. N.; Gangasharan, Nayak, S. K. *J. Chem. Soc., Faraday Trans. 2* **1993**, *89*, 509.
(55) (a) Davidson, D. W.; Wilson, G. J. *Can. J. Chem.* **1975**, *53*, 2215. (b) Gough, S. R.; Ripmeester, J. A.; Davidson, D. W. *Can. J. Chem.* **1975**, *53*, 2215.
(56) Hawkins, R. E.; Davidson, D. W. *J. Phys. Chem.* **1966**, *70*, 1889.
(57) Haida, O.; Matsuo, T.; Suga, H.; Seki, S. *J. Chem. Thermodyn.* **1974**, *6*, 815.
(58) Yamamuro, O.; Oguni, M.; Matsuo, T.; Suga, H. *J. Phys. Chem. Solids* **1987**, *48*, 935.
(59) Gough, S. R.; Davidson, D. W. *J. Chem. Phys.* **1970**, *52*, 5442.
(60) Kawada, S. *J. Phys. Soc. Jpn.* **1978**, *44*, 1881.
(61) Bjerrum, N. *Science* **1952**, *115*, 385.
(62) Murthy, S. S. N. *J. Phys. Chem.* **1989**, *93*, 3347.